NUWC-NL Technical Report 10,115
8 September 1992

(2)

Application of Biot Theory to the Study of Acoustic Reflection from Sediments

Dmitry Chizhik
J. Matthew Tatersall
Environmental and Tactical Support Systems Department

Naval Undersea Warfare Center Detachment
New London, Connecticut

PREFACE

This project was performed under NUWC Project No. A29405, the Principal Investigator is R. J. Christian (Code 3112), and Program Manager is F. A. Alatalo (Code 33A). The sponsoring activity is the Naval Sea Systems Command (PMO424 and 06UR1).

REVIEWED AND APPROVED: 8 September 1992

G. M. Mayer
Head: Environmental and Tactical
Support Systems Department

REPORT DOCUMENTATION PAGE

Form Approved
OMB No. 0704-0188

1. AGENCY USE ONLY (Leave blank)	2. REPORT DATE	3. REPORT TYPE AND DATES COVERED
	8 September 1992	

4. TITLE AND SUBTITLE

Application of Biot Theory to the Study of Acoustic Reflection from Sediments

5. FUNDING NUMBERS

PR A29405

6. AUTHOR(S)

Dmitry Chizhik and J. Matthew Tattersall

7. PERFORMING ORGANIZATION NAME(S) AND ADDRESS(ES)

Naval Undersea Warfare Center Detachment
New London, CT 06320

8. PERFORMING ORGANIZATION REPORT NUMBER

TR 10,115

9. SPONSORING/MONITORING AGENCY NAME(S) AND ADDRESS(ES)

Naval Sea Systems Command (PM0424 and 06UR1)
Naval Sea Systems Command Headquarters
Washington, DC 20362-5101

10. SPONSORING/MONITORING AGENCY REPORT NUMBER

11. SUPPLEMENTARY NOTES

12a. DISTRIBUTION/AVAILABILITY STATEMENT

Approved for public release; distribution unlimited.

12b. DISTRIBUTION CODE

13. ABSTRACT *(Maximum 200 words)*

Wave Propagation in fluid-saturated poroelastic media may be described using the theory developed by M. A. Biot between 1941 and 1962. The treatment is phenomenological and encompasses a wide range of physical mechanisms that affect the acoustic properties of porous media. Novel aspects of the theory are the prediction of a second "slow" compressional wave, frequency dispersion of compressional and shear wave velocities, and an attenuation that is not linearly dependent on frequency. These predictions have been experimentally confirmed only relatively recently. Biot theory may also be used for prediction of reflection and transmission of acoustic waves at a fluid-porous media boundary. (Cont'd)

14. SUBJECT TERMS

Acoustic Reflection
Biot Theory
Bottom Loss
Longitudinal Wave
Medium Sand Sediment

15. NUMBER OF PAGES

16. PRICE CODE

17. SECURITY CLASSIFICATION OF REPORT	18. SECURITY CLASSIFICATION OF THIS PAGE	19. SECURITY CLASSIFICATION OF ABSTRACT	20. LIMITATION OF ABSTRACT
UNCLASSIFIED	UNCLASSIFIED	UNCLASSIFIED	SAR

(Abstract Cont'd)

In this work, wave propagation in fluid-saturated, porous media are reviewed. Examples of velocity and attenuation dispersion as functions of frequency are shown. The ocean bottom reflection coefficient for a medium sand bottom computed using the Biot theory as functions of grazing angle and frequency is compared against the more common fluid-fluid and fluid-solid interface models. Finally, shallow water propagation loss measurements are compared with model results using Biot theory to predict frequency-dependent bottom loss. Good agreement with measured data is found at all frequencies considered, from 100 to 8000 Hz.

TABLE OF CONTENTS

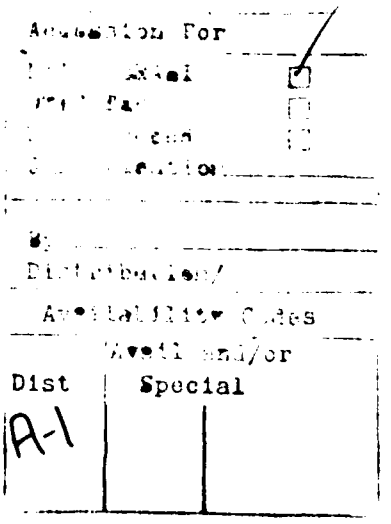

LIST OF ILLUSTRATIONS

APPLICATION OF BIOT THEORY TO ACOUSTIC REFLECTION FROM SEDIMENTS

INTRODUCTION

As an acoustic wave is reflected from the sea floor, some of the incident energy is lost in coupling to waves in the bottom and the inherent loss in the sediment. In shallow water, a transmitted acoustic signal typically suffers many bottom reflections before it is detected by a receiver. An error in the estimate of bottom loss of as little as 0.5 dB will accumulate to a 10 dB error in total propagation loss after only 20 reflections from the bottom. It is, therefore, important to develop realistic physical models of the acoustic properties of sediments in order to accurately predict propagation loss.

The problem considered in this work is that of a reflection of a plane acoustic wave incident from a constant velocity fluid half-space onto a homogeneous bottom half-space.

Conventionally, the sea bottom is modelled as either a lossy fluid or a viscoelastic solid. The fluid model only considers the propagation of compressional waves in the sediment and requires the knowledge of sediment mass density and the velocity and attenuation of compressional waves. This model is most appropriate for low-rigidity, unconsolidated sediments such as ooze, clay or silt.

The solid model is more accurate in that it includes the effect of sediment rigidity and thus requires the knowledge of both shear and compressional wave velocities and attenuations as well as the sediment mass density.

Both of these models usually assume a velocity that is independent of frequency and an attenuation that increases linearly with frequency. These assumptions result in frequency independent bottom loss.

More accurately, the sediment on the sea bottom may be viewed as a fluid saturated porous solid. This view is quite general and includes oozes, clays, silts, sands and porous rock such as sandstone. When the sediment is subjected to an acoustic disturbance, the solid frame of the sediment and the pore fluid oscillate separately and interact via inertial coupling as well as viscous drag. These mechanisms affect the acoustic wave propagation in ways not predicted by the simple homogeneous fluid or solid models.

Wave propagation in fluid-saturated, poroelastic media may be described using the theory developed by M.A. Biot between 1941 and 1962 [1]-[4]. The treatment is phenomenological and encompasses a wide range of physical mechanisms that affect the acoustic properties of porous media. Novel aspects of the theory are the prediction of a second "slow" compressional wave, frequency dispersion of compressional and shear wave velocities, and an attenuation that is not linearly dependent on frequency. These predictions have been experimentally confirmed only relatively recently [5]. Biot theory may also be used for prediction of reflection and transmission of acoustic waves at a fluid-porous media boundary.

In this work, wave propagation in fluid-saturated porous media will be reviewed. Examples of velocity and attenuation dispersion as functions of frequency will be shown. Ocean bottom reflection coefficient for a medium sand bottom computed using the Biot theory as a function of grazing angle and frequency will be compared against the more common fluid-fluid and fluid-solid interface models. Finally, shallow water propagation loss measurements will be compared with model results using Biot theory to predict frequency dependent bottom loss.

REVIEW OF BIOT THEORY

As mentioned in the introduction, the solid and the fluid parts of the sediment may be viewed as oscillating separately and interacting via inertial and viscous coupling mechanisms. Accordingly, the pore fluid dynamical relation will be discussed first. Then the dynamical relation for the entire fluid-solid aggregate will be stated. Using the viscoelastic stress-strain relations and separating the solution into rotational and irrotational fields, the longitudinal and shear wave equations may then be derived. The phase velocity and the intrinsic attenuation of plane monochromatic waves will then follow from the dispersion relations.

The dynamical relation for the fluid in the pore space may be expressed as

$$-\nabla p = \rho_f \frac{\partial^2 \mathbf{U}}{\partial t^2} + m_a \rho_f \frac{\partial^2 (\mathbf{U} - \mathbf{u})}{\partial t^2} + \frac{\eta F \beta}{k_s} \frac{\partial (\mathbf{U} - \mathbf{u})}{\partial t} \qquad (1)$$

where p is the fluid pressure in the pore, **U** is the displacement of the fluid and **u** is the displacement of the solid frame, ρ_f is the fluid mass density, η is the fluid static viscosity, and β and k_s are the porosity and the permeability of the sediment, respectively. The viscosity correction factor F will be discussed below. The second term on the right side of (1) accounts for the inertial coupling between the fluid and the solid, i.e., the fluid exerts a force against the walls of the pore space, thereby moving the solid frame. The added mass coefficient m_a is a measure of the tortuosity of pores. Note that, for uniform cross-section pores oriented parallel to the pressure gradient, the solid frame does not interfere with fluid motion and m_a is therefore equal to zero.

Viscous forces are important because of the large surface of interaction between the fluid and the solid. The last term in (1) represents the viscous drag force that forms the frictional coupling mechanism between the solid and the fluid. This term is an expression of Darcy's phenomenological law which states that under steady flow conditions the spatially averaged relative velocity of the fluid moving through a porous frame is proportional to the pressure gradient, i.e.,

$$-\nabla p = \frac{\eta \beta}{k_s} \frac{\partial}{\partial t} (\mathbf{U} - \mathbf{u})_{ave} .$$

Darcy's law also serves as the definition of permeability k_s. The above relation becomes invalid as the frequency increases. To include the higher frequency effects, Biot [2] has analyzed the microvelocity field in two simplified pore space geometries under oscillatory flow conditions and introduced the viscosity correction factor, F, which appears in (1). In the case of pores shaped as cylindrical capillary tubes oriented along the pressure gradient,

$$F = \frac{1}{4} \frac{\kappa\, T(\kappa)}{1 - 2T(\kappa)/i\kappa} \qquad (2)$$

$$T(\kappa) = \frac{ber'(\kappa) + i \cdot bei'(\kappa)}{ber(\kappa) + i \cdot bei(\kappa)} = \frac{-i\sqrt{i}\, J_1(i\sqrt{i}\kappa)}{J_0(i\sqrt{i}\kappa)}$$

$$\kappa = a_1 (\omega \rho_f / \eta)^{1/2}$$

where ber(κ) and bei(κ) are the real and imaginary parts of the Kelvin function [6], $J_1(z)$ and $J_0(z)$ are the Bessel functions of order one and zero, respectively [6], and ω is the radian frequency. The characteristic pore size parameter a_1 has been derived exactly for some idealized pore shapes; however, for real sediments, it is usually adjusted to match experimental data. Yamamoto and Turgut [7] have derived the viscosity correction factor for media characterized with a distribution of pore sizes. Application of their analysis, however, requires the additional knowledge of the standard deviation of the pore size distribution function, which is rarely available.

Defining the displacement of the solid relative to the fluid as $\mathbf{w} = \beta(\mathbf{u} - \mathbf{U})$, the fluid dynamical relation (1) may be rewritten as

$$-\nabla p = \rho_f \frac{\partial^2 \mathbf{u}}{\partial t^2} - c\frac{\rho_f}{\beta}\frac{\partial^2 \mathbf{w}}{\partial t^2} - \frac{\eta F}{k_s}\frac{\partial \mathbf{w}}{\partial t} \tag{3}$$

where the structure (or tortuosity) factor $c = 1 + m_a$. This parameter is also usually determined by matching model predictions to measured data in the case of real sediments.

The total force acting on the volume ΔV of the solid-fluid aggregate is

$$(\nabla \tau)\,\Delta V = \frac{\partial^2}{\partial t^2}(\rho_s \Delta V_s \mathbf{u} + \rho_f \Delta V_f \mathbf{U}) \tag{4}$$

$$\Delta V = \Delta V_s + \Delta V_f,$$

where τ_{ij} is the total stress tensor, ΔV_s and ΔV_f are the volumes of the parts of ΔV occupied by the fluid and the solid, respectively, and ρ_s is the mass density of the solid material alone. Note that as the stress τ_{ij} is the total stress tensor acting on both the fluid and solid constituents, no forces coupling the two need be included. Defining porosity β as $\beta = \Delta V_f / \Delta V$, the dynamical relation (4) may be rewritten as

$$\nabla \tau = \frac{\partial^2}{\partial t^2}(\rho \mathbf{u} + \rho_f \mathbf{w}) \tag{5}$$

$$\rho = \rho_s(1 - \beta) + \beta\rho_f,$$

where ρ is the mass density of the sediment.

The constitutive stress-strain relations may be expressed as

$$\tau = \mu \mathbf{e} + ((H - \mu)\,\nabla\cdot\mathbf{u} - C\,\nabla\cdot\mathbf{w})\,\mathbf{I} \tag{6}$$

$$p = M\,\nabla\cdot\mathbf{w} - C\,\nabla\cdot\mathbf{u},$$

where

$$e_{ij} = \frac{1}{2}\left(\frac{\partial u_i}{\partial x_j} + \frac{\partial u_j}{\partial x_i}\right).$$

In (6) e_{ij} is the strain tensor and I is the identity matrix. The elastic constants H, M and C have been related by Stoll [8] to K_b, K_r, and K_f, which are the bulk moduli of the porous frame, the solid material and the fluid, respectively,

$$\begin{aligned} H &= \frac{(K_r - K_b)^2}{D - K_b} + K_b + 4\mu/3 \\ C &= \frac{K_r(K_r - K_b)}{D - K_b} \\ M &= \frac{K_r^2}{D - K_b}, \end{aligned} \tag{7}$$

where $D = K_r(1+\beta(K_r/K_f - 1)$. In the above, μ is the rigidity of the solid frame. To allow for frame damping losses, K_b and μ are usually allowed to have small imaginary parts and are written as $K_b = K_b'(1+\delta)$ and $\mu = \mu'(1+\delta)$, where δ is the specific loss. Biot [3] has shown that the elastic constants H, C, M, and μ may actually be considered as operators in the time domain, or, equivalently, as frequency dependent quantities in the frequency domain. Such treatment would allow consideration of thermoelastic, electrochemical and other relaxation phenomena (Stoll [8]). This requires, however, an extensive and detailed analysis of the physical chemistry and thermodynamics of the fluid-saturated sediment to provide the relaxation times. In the absence of such knowledge, these quantities are assumed to be complex constants defined by (7). Stoll [8] suggests the following relationship between K_b' and μ'

$$K'_b = \frac{2\mu'(1+\sigma)}{3(1-2\sigma)},$$

where σ is the Poisson's ratio.

The wave equation may then be derived by substituting the constitutive relations (6) into the dynamical relations (3) and (5) and using definitions (7). Following Holland [9], the resulting wave equation may then be separated into the longitudinal and shear wave equations by expressing **u** and **w** in terms of scalar and vector potentials

$$\begin{aligned} \mathbf{u} &= \nabla \phi_s + \nabla \times \psi_s, \quad \nabla \cdot \psi_s = 0 \\ \mathbf{w} &= \nabla \phi_f + \nabla \times \psi_f, \quad \nabla \cdot \psi_f = 0 \end{aligned} \tag{8}$$

The longitudinal wave equations thus obtained are

$$H\nabla^2\phi_s - C\nabla^2\phi_f = \frac{\partial^2(\rho\,\phi_s - \rho_f\,\phi_f)}{\partial t^2}$$

$$C\nabla^2\phi_s - M\nabla^2\phi_f = \rho_f\frac{\partial^2\phi_s}{\partial t^2} - c\frac{\rho_f}{\beta}\frac{\partial^2\phi_f}{\partial t^2} - \frac{\eta F}{k_s}\frac{\partial\phi_f}{\partial t} \qquad (9)$$

Assuming monochromatic plane wave solutions of the form $\phi_s = A \exp i(\omega t - \mathbf{k}\cdot\mathbf{r})$, $\phi_f = B \exp i(\omega t - \mathbf{k}\cdot\mathbf{r})$, the longitudinal wave dispersion relation is obtained as

$$\begin{vmatrix} -k^2H + \omega^2\rho & k^2C - \omega^2\rho_f \\ -k^2C + \omega^2\rho_f & k^2M - \omega^2 m' \end{vmatrix} = 0 \qquad (10)$$

where $m' = c\,\rho_f/\beta - i\,\eta\,F/\omega\,k_s$. The phase velocity is defined as $v_L = \omega/k$. The intrinsic attenuation is defined as the imaginary part of the wave number k. The relative amplitudes and phases of potentials ϕ_s and ϕ_f may be found by substituting the values of v_L that are solutions to (10) into (9).

It is interesting to note that the above dispersion relation yields two solutions for the velocity v_L. One of these solutions corresponds to the usual compressional wave found in nonporous media. It is called Type I longitudinal wave, and its velocity and attenuation are plotted in figures 1 and 2 as functions of frequency for medium sand sediment. The values of material parameters are listed in table 1 and discussed in the section on measurements. Note that the velocity is dispersive and that the assumption that high frequency measurements of velocity, often carried out at 400 kHz, apply at low frequencies leads to an error of 100 m/s (Hamilton [10]). Also, the intrinsic attenuation of this wave does not vary linearly with frequency, as is commonly assumed [10]. Under Type I excitation, the fluid and the solid move essentially in phase.

The velocity and attenuation of the second compressional wave are plotted versus frequency in figures 3 and 4. This wave, called Type II, or "slow," longitudinal wave, is extremely lossy at low frequencies and becomes significant only at higher frequencies. Plona [5] reported detecting this wave in a laboratory at 500 kHz. For this wave, the fluid and the solid displacements are comparable in amplitude and essentially out of phase, i.e., the relative displacement, w, is large. As may be seen from equation (3), the viscous force term increases with w, and the energy of the wave is quickly dissipated. As the frequency is increased, the inertial terms in equation (3) become more significant, and the solution becomes a propagating rather than a diffusive wave. Calculations carried out in this work for the medium sand bottom parameters shown in table 1, as well as those carried out by Holland [9] for carbonate sand, indicate that the amount of incident acoustic energy converted into Type II longitudinal waves at the water-sand interface is extremely small.

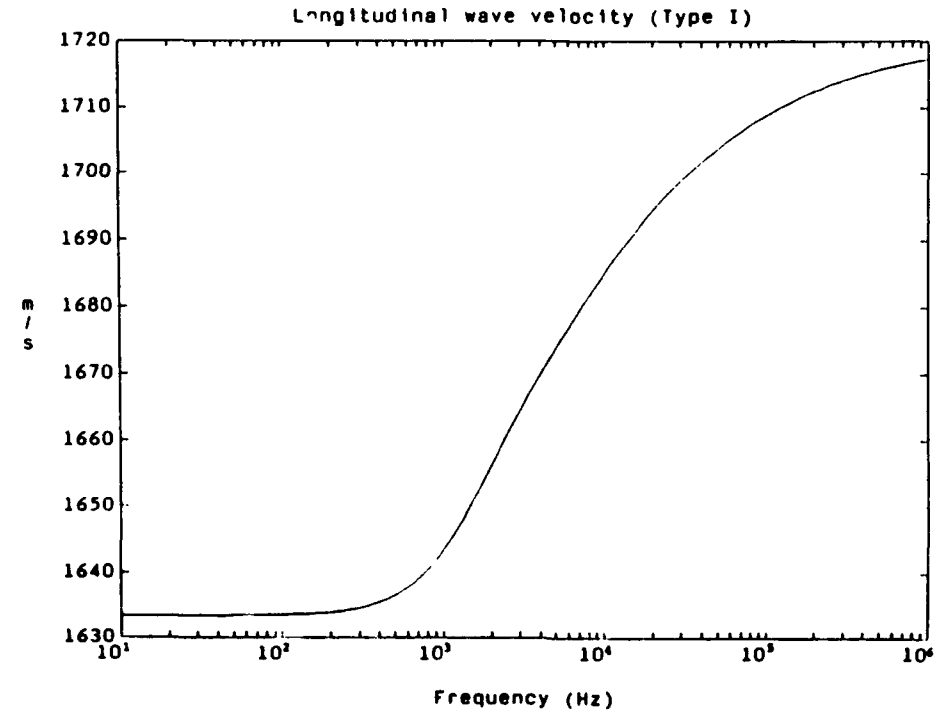

Figure 1. Velocity of Type I Longitudinal Wave in the Medium Sand Sediment as a Function of Frequency
(The sound speed ratio at the interface may be calculated using the sound velocity of 1524 m/s in water.)

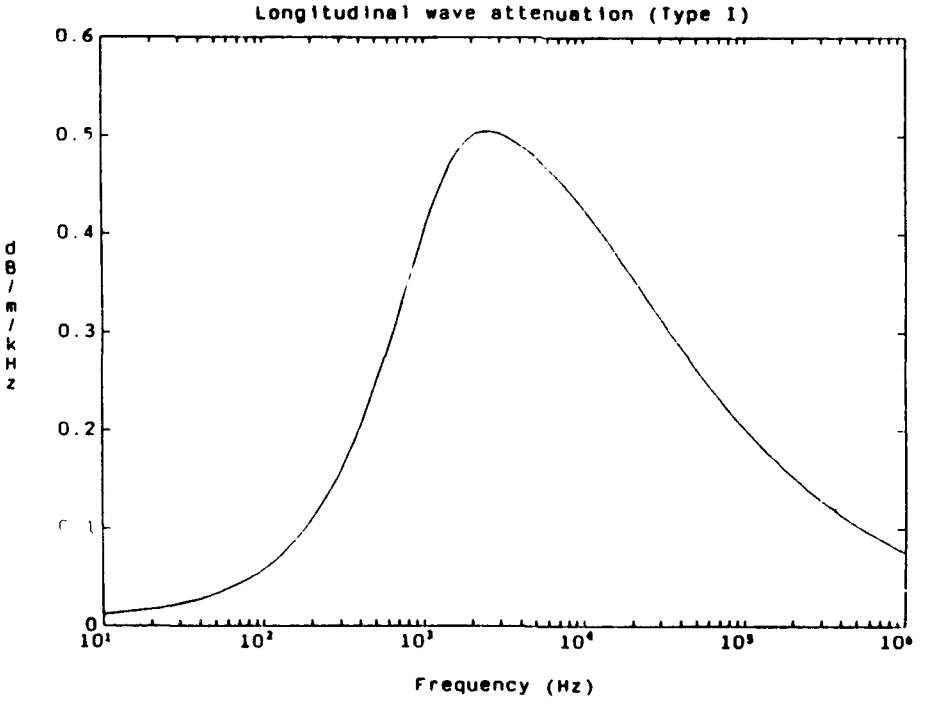

Figure 2. Intrinsic Attenuation of Type I Longitudinal Wave in the Medium Sand Sediment as a Function of Frequency

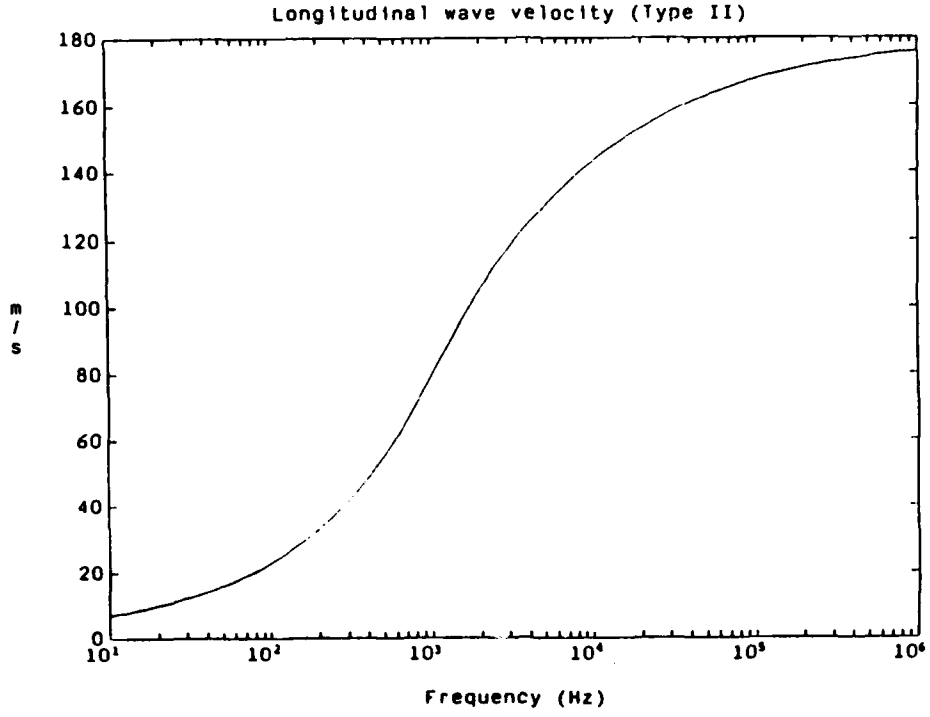

Figure 3. Velocity of Type II Longitudinal Wave in the Medium Sand Sediment as a Function of Frequency

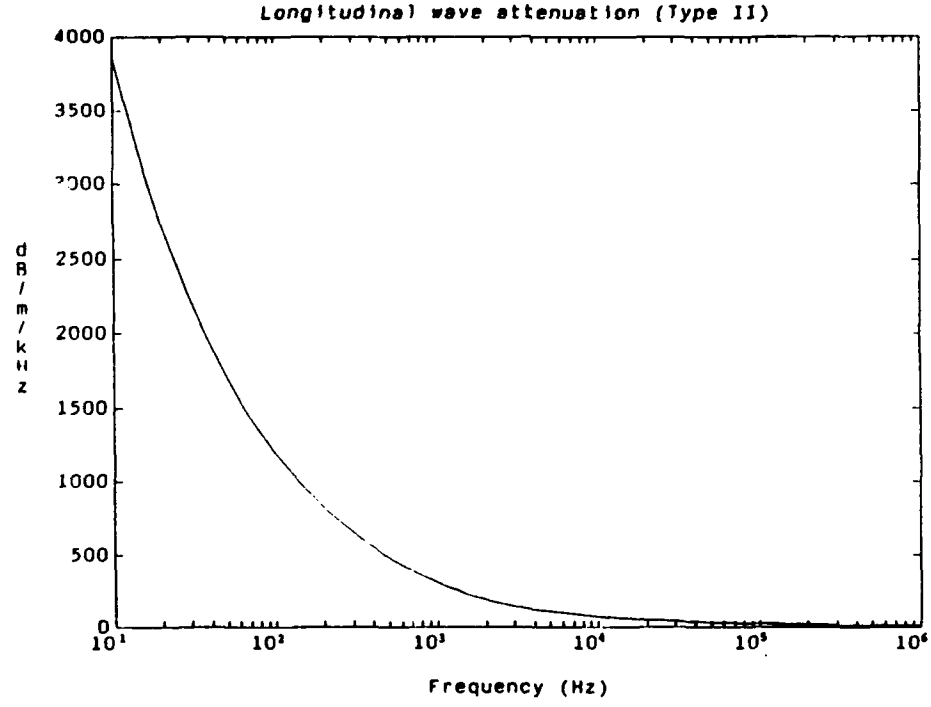

Figure 4. Intrinsic Attenuation of Type II Longitudinal Wave in the Medium Sand Sediment as a Function of Frequency

Analogously, the shear wave equations may be derived as

$$\mu \nabla^2 \psi_s = \rho \frac{\partial^2 \psi_s}{\partial t^2} - \rho_f \frac{\partial^2 \psi_f}{\partial t^2}$$

$$0 = \rho_f \frac{\partial^2 \psi_s}{\partial t^2} - c \frac{\rho_f}{\beta} \frac{\partial^2 \psi_f}{\partial t^2} - \frac{\eta F}{k_s} \frac{\partial \psi_f}{\partial t} \qquad (11)$$

And the shear wave dispersion relation is

$$v_s = \sqrt{\frac{\mu}{\rho - \rho_f^2 / m'}} \qquad (12)$$

where m' is the same as in equation (10). This relation has one solution, and the resulting shear wave velocity and attenuation are plotted versus frequency in figures 5 and 6. Note that, once again, the velocity is dispersive and that the attenuation does not increase linearly with frequency.

Table 1. Fluid and Medium Sand Sediment Properties Used in Calculations Involving the Biot Model

Parameter	**Value**	**Units**
Fluid density (ρ_f)	1024	kg/m^3
Fluid bulk modulus (K_f)	2.38×10^{10}	N/m^2
Fluid viscosity (η)	1.01×10^{-3}	kg/ms
Grain density (ρ_r)	2650	kg/m^3
Grain bulk modulus (K_r)	3.6×10^{10}	N/m^2
Porosity (β)	0.43	
Permeability (k_s)	1.25×10^{-11}	m^2
Structure factor (c)	1.75	
Pore size (a_1)	30×10^{-6}	m
Poisson's ratio (σ)	0.2	
Frame shear bulk modulus (μ_b)	$5 \times 10^7 (1 + i\, 0.02)$	N/m^2

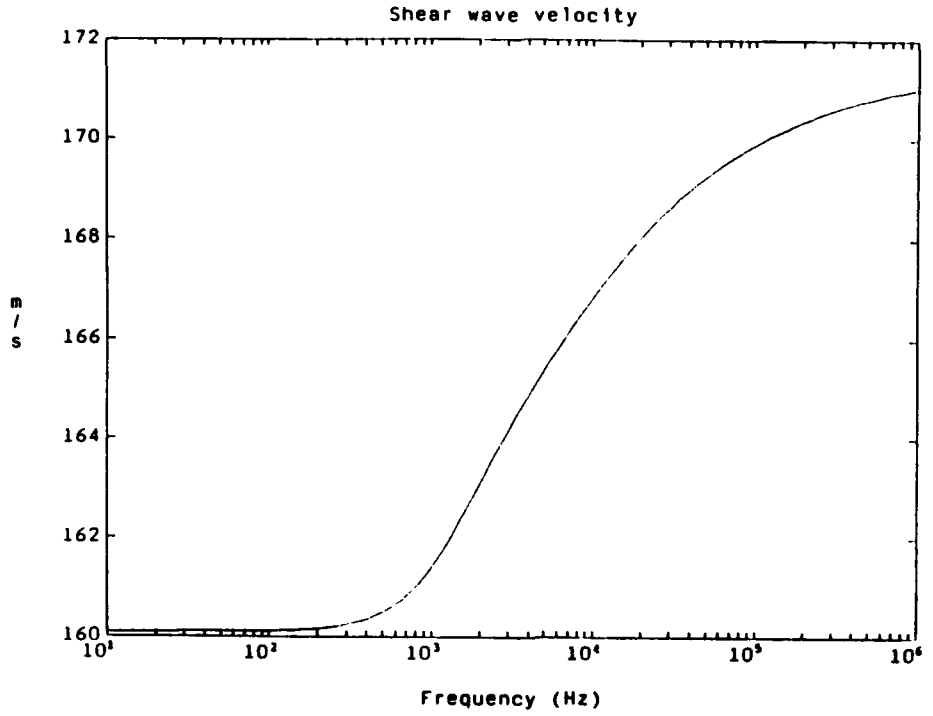

Figure 5. Velocity of a Shear Wave in the Medium Sand Sediment as a Function of Frequency

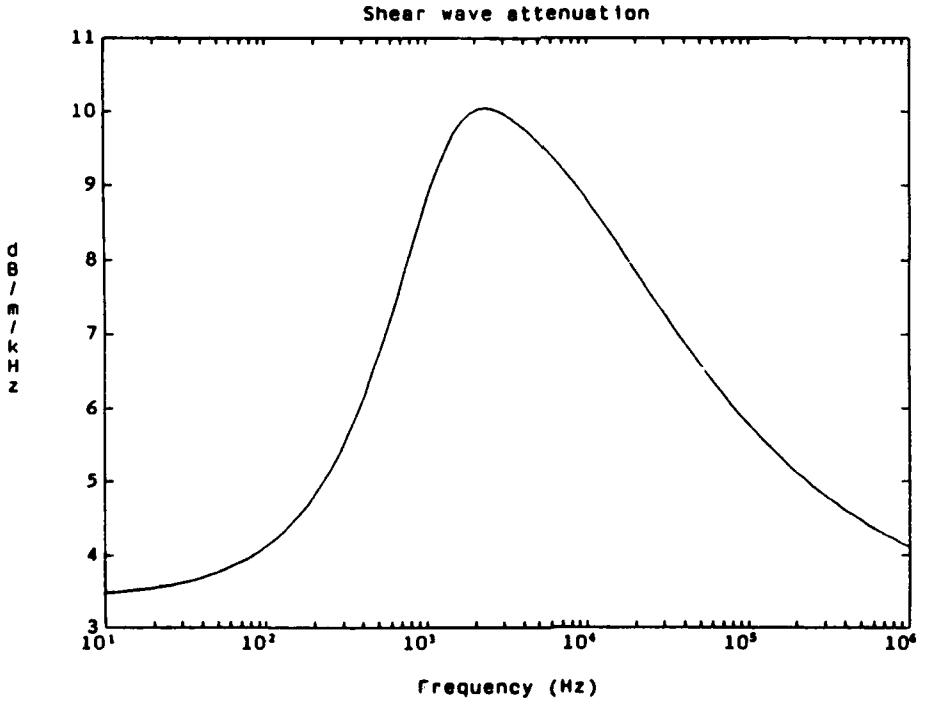

Figure 6. Intrinsic Attenuation of a Shear Wave in the Medium Sand Sediment as a Function of Frequency

BOTTOM LOSS PREDICTION

Stoll and Kan [11] and later Wu, et. al., [12] have evaluated the reflection coefficient for a plane wave incident from the fluid half-space onto a porous solid. Holland [9] has derived a relatively concise expression for the reflection and transmission coefficients. The field in the water above the interface consists of the incident and reflected longitudinal waves, while below the interface the field is the superposition of the transmitted Type I and Type II longitudinal waves and the shear wave. The relative amplitudes and phases of these waves may be found by matching the boundary conditions, thus providing the plane wave reflection and transmission coefficients. The boundary conditions for the fluid-porous solid interface may be stated as the continuity of normal particle displacement and normal stress and zero tangential stress. Since in porous media there are two displacement fields, **u** and **w**, instead of the usual one, an additional boundary condition is necessary. Assuming that, at the interface, the fluid is free to move in and out of the pores (open pore boundary condition), the fluid pressures in the pores and above the interface are set to be equal.

The amplitude of the pressure reflection coefficient |R|, expressed as bottom loss (-20 log10 |R|), was calculated at several frequencies using the parameters shown in table 1, which were chosen as representative of medium sand. The result is plotted versus grazing angle in figure 7. Note that, unlike the conventional models, Biot theory predicts a strong frequency dependence of the bottom loss at shallow grazing angles which are of interest in long range propagation.

Bottom loss calculated using the Biot theory as well as that using the fluid sediment model are compared in figure 8. Note that, at shallow grazing angles, the disagreement between the two models reaches 0.5 dB. The agreement is somewhat better between the solid model and the Biot theory result as can be seen in figure 9. It should be pointed out that, in calculating bottom loss using the fluid as well as the solid models of the sediment, the velocities and attenuations of the longitudinal and shear waves were determined using Biot theory. If these parameters were determined using the conventional assumptions, the differences with the Biot theory would have been more significant, especially at low frequencies.

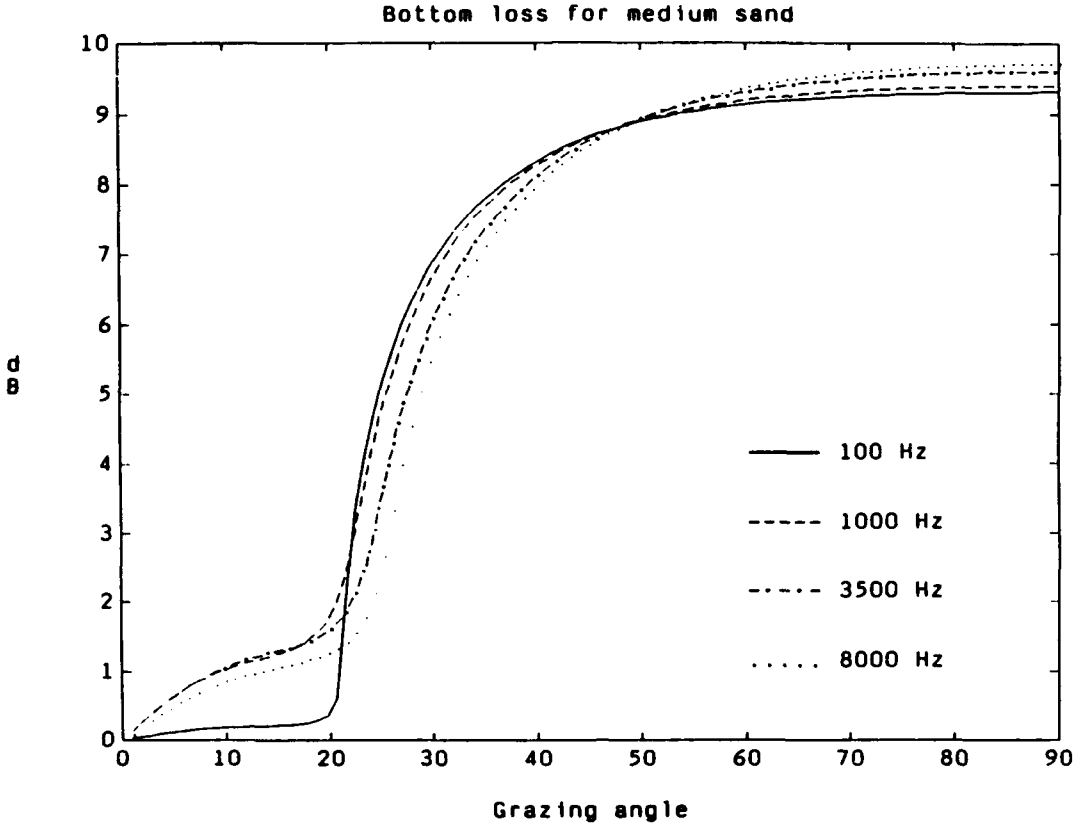

Figure 7. Bottom Loss as a Function of Grazing Angle for Medium Sand Calculated Using the Biot Theory for Several Frequencies

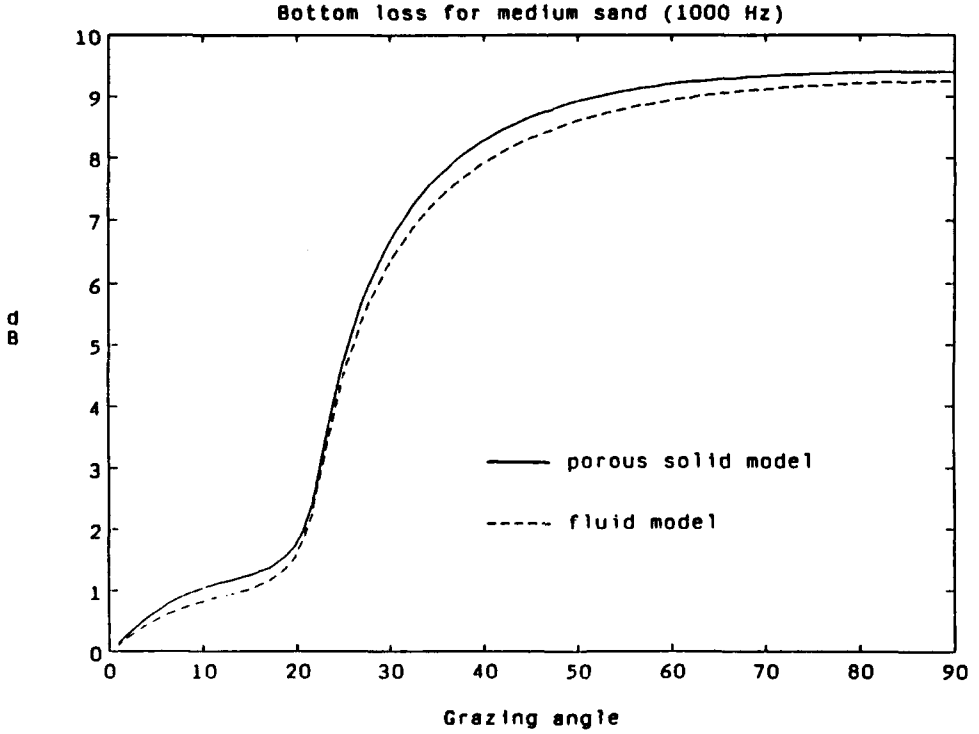

Figure 8. Bottom Loss for Medium Sand at 1000 Hz as a Function of Grazing Angle Calculated Using Both the Biot and the Fluid Models of the Sediment

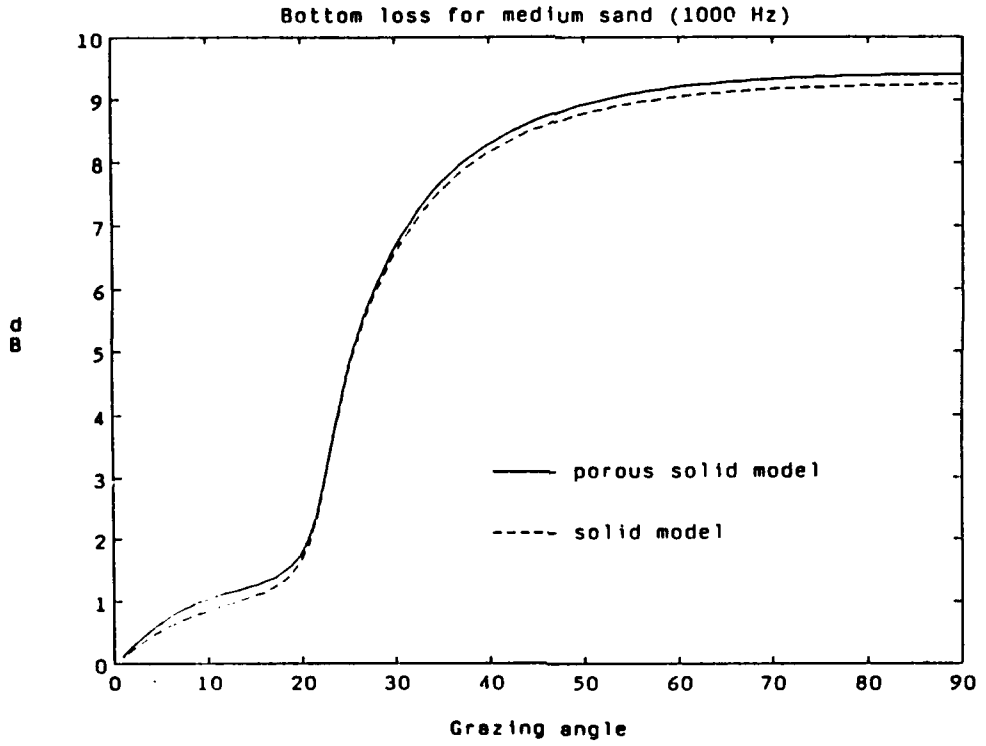

Figure 9. Bottom Loss for Medium Sand at 1000 Hz as a Function of Grazing Angle Calculated Using Both the Biot and the Solid Models of the Sediment

PROPAGATION LOSS MEASUREMENTS AND DETERMINATION OF PARAMETERS

To test the model predictions, propagation loss data collected in May of 1967 in shallow waters south of Long Island [13] were used. The measurements were carried out with a wide-band (explosive) source under downward-refracting conditions which occur in the presence of a negative sound velocity gradient. The source and the receiver were placed sufficiently deep so as to minimize the interaction with the sea surface.

In determining the parameters in table 1, the acoustic velocity, the mass density, and the viscosity of the fluid near the bottom were based on bathythermographic measurements as well as tabulated properties of water. The fluid bulk modulus K_f may be found from $v_f = (K_f/\rho_f)^{1/2}$. The saturated density of sediment and average grain size were determined from core sample measurements taken in the area. As the sediment was found to be medium-grain-size quartz sand, porosity and the pore size parameter were calculated (Stoll [8]). The mass density and the bulk modulus of the individual grains were taken to be that of quartz. The shear modulus, μ, of the solid frame is a function of overburden pressure which increases with depth, as discussed by Stoll [8]. In this work, a homogeneous porous half-space is considered for simplicity, and thus an effective value of μ',suggested by Yamamoto [14], is used. Poisson's ratio σ of 0.2 is used to determine K_b' (Stoll [8]). The value of permeability was taken from Yamamoto [14] and adjusted slightly to fit the propagation loss data. Such an adjustment is permissible because permeability varies with location and sediment type. Once the Biot parameters shown in table 1 were selected, they were used for predictions of bottom loss at all frequencies.

To predict propagation loss, a multipath expansion propagation model [15] was used. The sound velocity profile in the water column was taken from bathythermographic measurements and values for bottom loss were calculated using the Biot theory as described above. It should be noted that for a large receiver-transmitter separation, the arriving eigenrays interact with the bottom at only a narrow range of shallow grazing angles, with a beam width of about 20°.

The resulting predictions of propagation loss are compared against measurements for a number of frequencies in figures 10-13. Also shown are the predictions using the same propagation model under the conventional assumption of a fluid bottom with a dispersionless velocity and an attenuation that increases linearly with frequency [16]. It may be observed that both models perform reasonably well for the higher frequencies of 500 Hz, 3500 Hz, and 8000 Hz. (The fluid model prediction at 8000 Hz was compared with measurements by Cohen and Cole [13] and found to match the data well.) In the May 1991 analysis, transmission loss data taken at 1000 Hz at the same site indicated that both models give good agreement with the measurements [17]. At 100 Hz, however, the fluid bottom model overestimates the bottom loss significantly [18], and the Biot model is still in agreement with measurements. This agreement is to be expected because the Biot model predicts a much smaller bottom loss at shallow grazing angles at 100 Hz than at higher frequencies, as may be seen in figure 7. The fluid model, on the other hand, predicts a bottom loss that is independent of frequency, clearly in disagreement with the measurements.

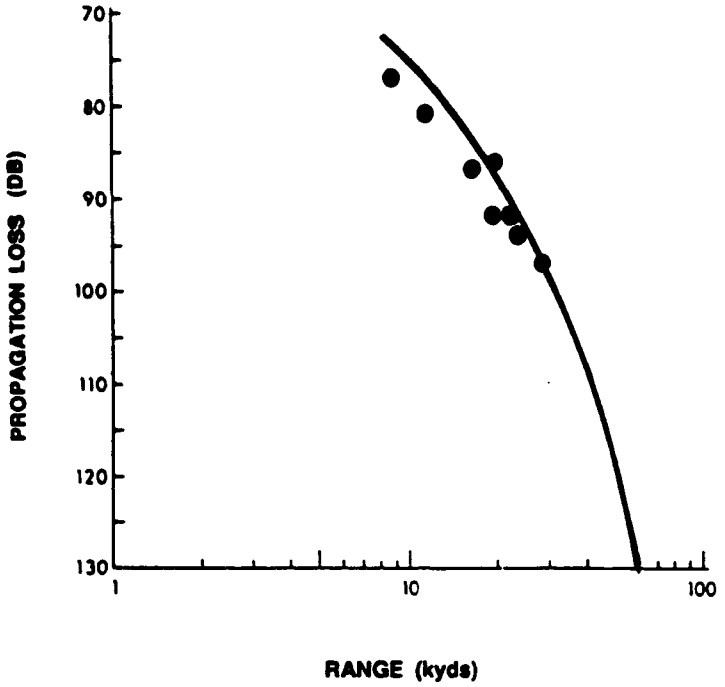

Figure 10. Propagation Loss at 8000 Hz as a Function of Range
(Measured data is shown as solid circles and the Biot theory prediction is shown as a solid line.)

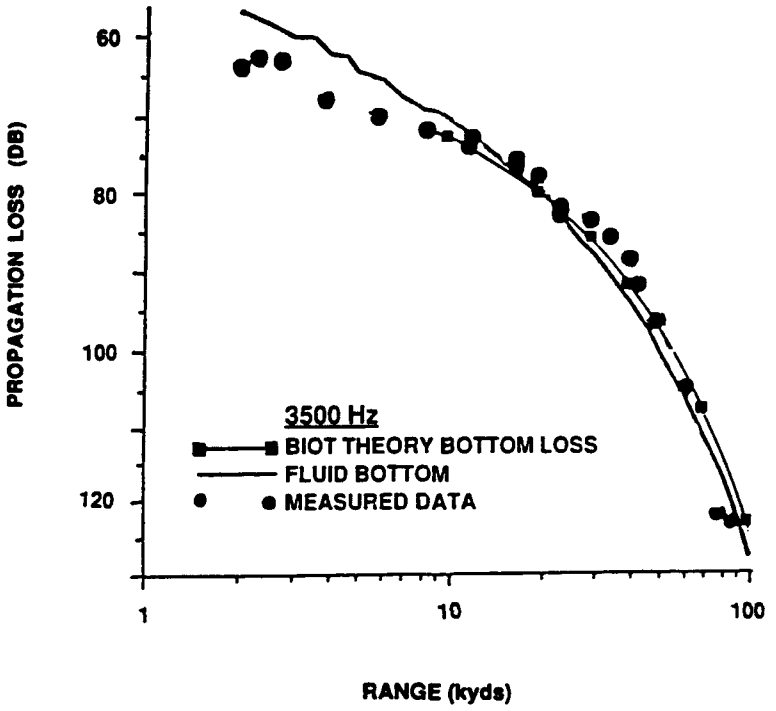

Figure 11. Propagation Loss at 3500 Hz as a Function of Range

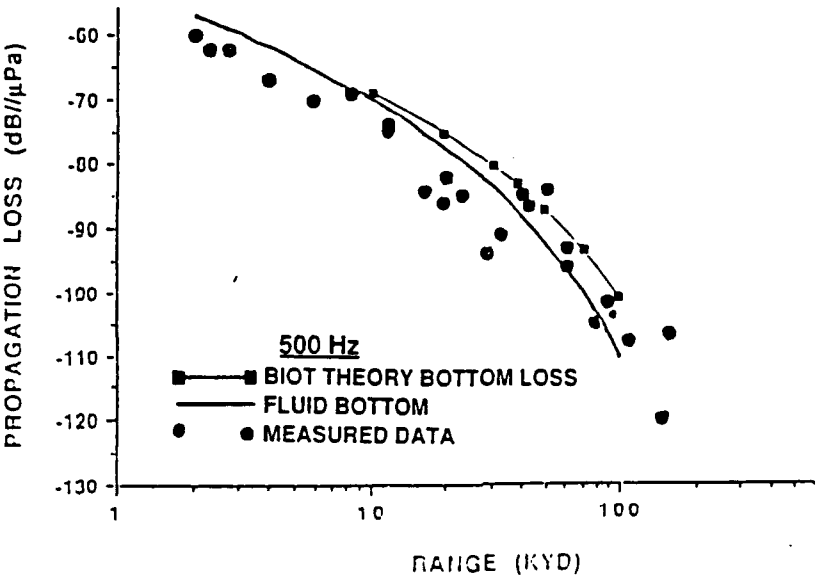

Figure 12. Propagation Loss at 500 Hz as a Function of Range

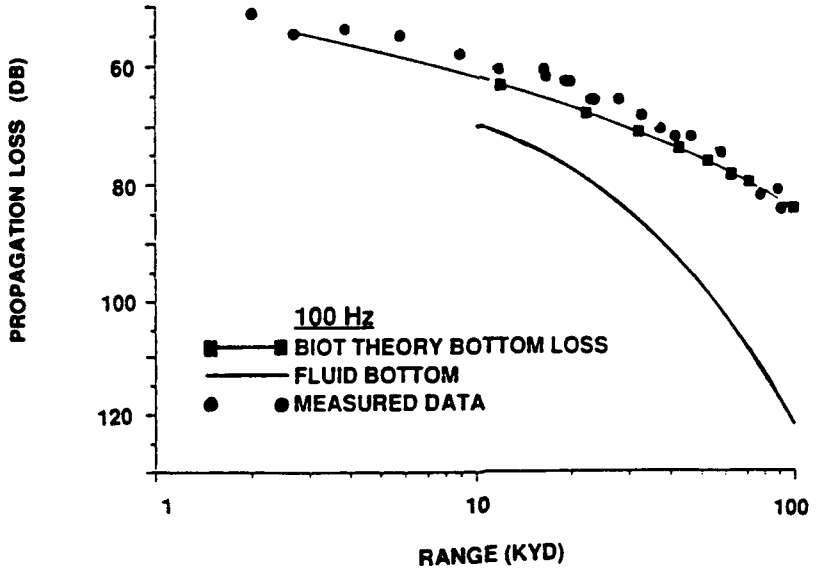

Figure 13. Propagation Loss at 100 Hz as a Function of Range

SUMMARY AND CONCLUSIONS

Biot theory of acoustic wave propagation in fluid saturated porous media was applied to bottom loss prediction for a sea bottom consisting of medium sand. The theory predicts a frequency-dependent bottom loss in contrast to the fluid or solid bottom models. Propagation loss predicted with the Biot model of the sediment showed agreement with measurements at frequencies ranging from 100 to 8000 Hz. The fluid model, which assumed a dispersionless velocity and an attenuation that is proportional to frequency, has performed poorly at low frequency (100 Hz).

As the Biot theory includes phenomena not considered in the simple fluid or solid models. it requires more detailed knowledge of the sediment and, thus, more parameters. Once these parameters are determined, however, bottom loss may be predicted at a broad range of frequencies, which makes this model superior to the conventional ones.

Since many algorithms and analytic methods used in underwater acoustics assume a simple fluid or solid bottom, it may be useful to approximate the sediment as a 'Biot' fluid or a 'Biot' solid with the velocities and attenuations of longitudinal and shear waves obeying the frequency dependence predicted by the Biot theory.

Biot theory has also been used by Yamamoto [14] in normal mode solutions to the shallow water acoustic waveguide. The water column was assumed to be isovelocity, and bottom half-space was assumed to be homogeneous.

Further work should include the variation of sediment physical properties with depth to simulate the bottom response more closely. This variation may significantly affect bottom response, as indicated by Hamilton [10], who reported large compressional and shear wave velocity gradients near the sediment-water interface. Badiey and Yamamoto [19] have investigated theoretically the effect of shear rigidity variation with depth on normal mode propagation in a shallow water wave guide. They also considered the effect of anisotropy induced by sediment layering. More data are necessary to determine the needed sediment parameters.

REFERENCES

[1] M. A. Biot, "Theory of Propagation of Elastic Waves in a Fluid-Saturated Porous Solid. I. Low-Frequency Range," Journal of the Acoustical Society of America, vol. 28, no. 2, 1956, pp. 168-178

[2] M. A. Biot, "Theory of Propagation of Elastic Waves in a Fluid-Saturated Porous Solid. II. Higher-Frequency Range," Journal of the Acoustical Society of America, vol. 28, no.2, 1956, pp.179-191.

[3] M. A. Biot, "Mechanics of Deformation and Acoustic Propagation in Porous Media," Journal of Applied Physics, vol. 33, no. 4, 1962, pp. 1482-1498.

[4] M. A. Biot, "Generalized Theory of Acoustic Propagation in Porous Media," Journal of the Acoustical Society of America, vol. 34, no. 9, 1962, pp. 1254-1264.

[5] T. J. Plona, "Observation of a Second Bulk Compressional Wave in a Porous Medium at Ultrasonic Frequencies," Applied Physics Letter, vol. 36no. 4, 1980, pp. 259-261.

[6] M. Abramovitz and I. A. Stegun, "Handbook of Mathematical Functions," Dover, New York, 1970.

[7] T. Yamamoto and A. Turgut, "Acoustic Wave Propagation Through Porous Media with Arbitrary Pore Size Distributions", Journal of the Acoustical Society of America, vol.83,no. 5, 1988, pp. 1744-1751.

[8] R. D. Stoll, "Sediment Acoustics," Lecture Notes in Earth Sciences, vol. 26, Springer-Verlag (1989)

[9] C. W. Holland, "The Effects of Sediment Porosity on Acoustic Reflection and Transmission at the Seafloor", Ph. D. Dissertation, The Pennsylvania State University, 1991.

[10] E. L. Hamilton, "Geoacoustic Modelling of the Sea Floor," Journal of the Acoustical Society of America, vol. 68, no.5, 1980, pp.1313-1340.

[11] R. D. Stoll and T.-K. Kan, "Reflection of Acoustic Waves at Water-Sediment Interface", Journal of the Acoustical Society of America, vol. 70,no. 1, 1981,pp. 149-156.

[12] K. Wu, Q. Xue, and L. Adler, "Reflection and Transmission of Elastic Waves from Fluid-Saturated Porous Solid Boundary", Journal of the Acoustical Society of America, vol. 87,no. 6, 1990, pp. 2349-2358.

[13] J. S. Cohen and B. F. Cole, "Shallow Water Propagation Under Downward-Refraction Conditions. II," Journal of the Acoustical Society of America, vol. 61,no. 1, 1977,pp. 213-217.

[14] T. Yamamoto, "Acoustic Propagation in the Ocean with a Poroelastic Bottom," Journal of the Acoustical Society of America, vol. 73, no. 5, 1983, pp.1587-1596.

[15] H. Weinberg, "Application of Ray Theory to Acoustic Propagation in Horizontally Stratified Oceans," Journal of the Acoustical Society of America, vol. 58, no. 1,1975, pp. 97-109.

[16] B. F. Cole and E. M. Podeszwa, "Shallow-Water Propagation Under Downward-Refraction Conditions," Journal of the Acoustical Society of America, vol. 41, no. 6, 1967, pp. 1479-1484.

[17] J. M. Tattersali, D. Chizhik, and K. L. Francis, "Frequency Dependent Reflectivity of a Medium Sand Bottom in Shallow Water Inferred from Transmission Loss Measurements", NUWC-NL Technical Memorandum 921115, Naval Undersea Warfare Center, New London, CT, in review.

[18] J. A. Davis, B. F. Cole, P. D. Herstein, S. R. Santaniello, and W. M. Leen, unpublished report.

[19] M. Badiey and T. Yamamoto, "Propagation of Acoustic Normal Modes in a Homogeneous Ocean Overlaying Layered Anisotropic Porous Beds," Journal of the Acoustical Society of America, vol. 77, no. 3,1985, pp. 954-961.

INITIAL DISTRIBUTION LIST

Addressee	No. of Copies
ARL/UT (J. Shooter, S. Mitchell, N. Bedford, E. Westwood, Library)	5
BBN/Cambridge (G. Shepard)	1
BBN/New London (P. Cable)	1
DARPA (W. Carey)	1
DTIC	2
LDGO (R. Stoll)	1
NAVSEA (PMO 424, 06UR1)	1
ONR R. Feden (124), K. Dial, E. Chaika, E. Estalotte, B. Blumenthal, M. Orr)	6
ONR Det/Bay St. Louis (D. Small)	1
NRL (F. Erskine, O. Diachok, M. Czarnecki, Library)	4
NRL/NSTL (B. Adams, E. Franchi, J. Matthews, P. Bucca, J. Caruthers, Library)	6
NAVOCEANO (R. Merrifield (PMI), R. Christensen (OA))	2
NAWC (B. Steinberg (5031))	1
PSI/McLean (C. Holland)	1
PSI/NL (J. Davis, S. Santaniello)	2
SAIC/McLean (R. Dicus, A. Eller, C. Spofford, R. Cavanaugh)	4
SAIC/NL (F. DiNapoli, D. Griffiths, R. Evans, M. Fecher, J. Hanrahan)	5
TRACOR (S. Reilly, G. Heines)	2
WHOI (G. Frisk, G. M. Purdy)	2
SCHLUMBERGER-DOLL (T. Plona)	1